Electronics and Electrical Engineering

AIMS Electronics and Electrical Engineering, 8(2): 265–291.
DOI: 10.3934/electreng.2024012
Received: 28 March 2024
Revised: 07 May 2024
Accepted: 14 May 2024
Published: 22 May 2024

https://www.aimspress.com/journal/ElectrEng

Research article

Integration of predictive and computational intelligent techniques: A hybrid optimization mechanism for PMSM dynamics reinforcement

Shaswat Chirantan* and Bibhuti Bhusan Pati

Department of Electrical Engineering, Veer Surendra Sai University of Technology, Burla, Sambalpur, 768018, India

* **Correspondence:** Email: shaswat.chirantan443@gmail.com.

Abstract: This paper presents an integrated approach combining a sequential neural network (SNN) with model predictive control (MPC) to enhance the performance of a permanent magnet synchronous motor (PMSM). We address the challenges of traditional control methods that struggle with the dynamics and nonlinear nature of PMSMs, offering a solution that leverages the predictive capabilities of MPC and the adaptive learning potential of neural networks. Our SNN-MPC model is contrasted with state-of-the-art genetic algorithm (GA) and ant colony optimization (ACO) methods through a comprehensive simulation analysis. This analysis critically examines the dynamic responses, including current, torque, and speed profiles, of the PMSM under proposed hybrid control strategies. The heart of the work deals with the optimal switching states and subsequent voltage injection to the inverter fed PMSM drive by a predefined minimization principle of a current modulated objective function, where MPC constitutes an integral finite control set (IFCS) mechanism for voltage vector selection and thereby selects the optimized integral gains K_d and K_q for direct and quadrature axes, respectively, with the FCS gain K_{fcs} obtained from implemented intelligent techniques. Based on the control criteria, the SNN-MPC scheme was established as the preferred benchmark with optimized tuning values of K_d = 0.01, K_q = 0.006, and K_{fcs} = 0.13, as compared to the gain values tuned from GA and ACO. The experimental setup utilized MATLAB and a Python environment for robust and flexible simulation, ensuring an equitable basis for comparison across all models.

Keywords: permanent magnet synchronous motor; model predictive control; genetic algorithm; ant colony optimization; sequential neural network; voltage source inverter; finite control set; integral finite control set

Abbreviations: MPC: model predictive control; PCC: predictive current control; FCS: finite control set; IFCS: integral finite control set; PMSM: permanent magnet synchronous motor; SVM: space vector modulation; VSI: voltage source inverter; IGBT: insulated gate bipolar transistor; SNN: sequential neural network; GA: genetic algorithm; ACO: ant colony optimization

List of Symbols

(i_d, i_q)	Components of stator current in ***(d, q)*** reference frame
(v_d, v_q)	Components of stator voltage in ***(d, q)*** reference frame
S_a, S_b, S_c	Switching states of the inverter
R_s	Winding resistance offered to stator
L_d, L_q	Inductance of direct and quadrature axes
J	Moment of inertia
B	Friction viscous gain
P	Number of poles
ω_s, ω_e	Stator and electrical speed
T_e, T_L	Electrical and load torque
V_{DC}	DC bus voltage
V_{aN}, V_{bN}, V_{cN}	Phase voltages
Φ_{mg}	Rotor flux
$i_d(t_{i+1}), i_q(t_{i+1})$	Predicted values of current in d-q frame
i_d^*, i_q^*	Desired values of current in d-q frame
T_S	Sampling Interval
Θ	Rotor angle position

1. Introduction

Permanent magnet synchronous motors (PMSMs) represent a significant advancement in electric motor technology [1,2], characterized by their use of permanent magnets embedded in or attached to the rotor. This design contributes to their high efficiency, compact size, and superior performance compared to traditional induction motors. PMSMs are widely utilized in various applications, including electric vehicles [3], industrial automation, robotics, and renewable energy systems, where high efficiency and precise control are paramount.

1.1. Background

The inherent advantages of PMSMs, such as their ability to operate at high speeds and their dynamic response capabilities, make them an ideal choice for applications demanding high performance and reliability. Controlling PMSMs presents unique challenges, primarily due to their complex dynamics and the need for precise control of torque and speed under varying operational conditions [4]. Achieving optimal performance [5] requires sophisticated control algorithms capable of adapting to changes in load and ensuring efficient operation throughout the motor's speed range. The complexity of PMSM control is further compounded by the nonlinear characteristics of the motor and the interaction between the magnetic fields of the stator and the permanent magnets on the rotor [6]. Traditional control algorithms, such as field-oriented control (FOC) and direct torque

control (DTC) [7,8], have been the cornerstone of PMSM control strategies [9–14]. In addition to this, inverter fed machine drive parameters can be regulated by duty cycle compensations [15,16] and lead to an optimal management of machine operation.

However, the quest for improved performance has led to the exploration of predictive control algorithms. These algorithms, including the genetic algorithm (GA) [17] and ant colony optimization (ACO) [20], offer advantages in terms of their ability to predict future states of the motor and adjust control actions accordingly. Predictive control algorithms aim to optimize the motor's performance by considering future operational scenarios, thereby enhancing efficiency, reducing energy consumption, and improving dynamic response. The sequential neural network model predictive control (SNN-MPC) model represents a novel approach in the realm of PMSM control. By integrating neural networks [17–19] with model predictive control [9–14], the SNN-MPC model aims to leverage the predictive capabilities of neural networks to enhance the accuracy and efficiency of control actions. This model stands out by its ability to adapt to changing conditions in real time, offering a significant improvement over traditional algorithms in terms of performance optimization and adaptability. The SNN-MPC model adapts quickly to changing motor conditions, providing real-time control with minimal oscillations and energy consumption. It offers improved adaptability and fault detection compared to GA and ACO. However, the framework requires significant computational resources for training and execution, which may limit its practicality in resource-constrained environments. Additionally, ongoing model tuning requires high-quality training data that represents diverse motor dynamics. GA and ACO, while less adaptable, are simpler and more efficient in computationally limited settings.

1.2. Literature review and research gap

In the evolving landscape of optimization techniques, particularly in the application to permanent magnet synchronous motors (PMSMs), a diverse array of studies have demonstrated the efficacy of integrating ant colony optimization (ACO), particle swarm optimization (PSO), and neural networks to enhance system performance and efficiency. Mao et al. [19] delved into the realm of neural network-based model predictive control for PMSMs, unveiling a strategy that significantly reduces overshoot by 5.87% and rise time by 0.036 s. Their model, which employs particle swarm optimization (PSO) to train echo state networks (ESN), showcases an innovative approach to stabilizing and accurately predicting motor speed, thereby optimizing predictive control and enhancing robustness against parameter variations and load disturbances. This study not only highlights the potential of neural networks in predictive control but also emphasizes the role of PSO in refining the training process for improved system response and stability.

Further extending the exploration of hybrid optimization methods, Valdez et al. [20] introduced a novel hybrid technique that amalgamates ACO and PSO, optimized for modular neural networks. This method, aimed at classifying images of human faces, outperforms traditional optimization techniques, underscoring the synergy between ACO and PSO in tackling complex optimization problems. On a different note, Saeed and Sheikhyounis [21] applied a combination of PSO and neural network techniques to enhance power quality in distribution systems, demonstrating a significant reduction in total harmonic distortion and an improvement in system resilience to power disturbances. Similarly, Chafi and Afrakhte’s [22] investigation into short-term electrical load forecasting [23] using neural networks and PSO algorithm presents a compelling case for the

accuracy and efficiency of these techniques in predicting electrical loads, thereby facilitating more effective power grid management.

These studies collectively underscore the versatility and effectiveness of ACO, PSO, and neural network-based optimization techniques [24–30] across various applications, from motor control [31,32] to power quality improvement and load forecasting. By leveraging these methods, researchers and practitioners can achieve substantial improvements in system performance, efficiency, and accuracy, paving the way for innovative solutions in the field of optimization and control systems.

1.3. Motivations

The review of the referred literature highlighted the strengths and weaknesses of various algorithms applied to machine drives and provides valuable insights into their suitability for different operational scenarios. The findings from this study underscore the potential of the SNN-MPC model to revolutionize PMSM control, offering a promising avenue for future research and development. The superior performance of the SNN-MPC model suggests that integrating neural networks with predictive control algorithms can significantly enhance motor control dynamics. Future research could focus on refining the SNN-MPC model, exploring other advanced control strategies, and applying these findings to real-world PMSM systems to fully realize their potential benefits. The evolution of PMSM control strategies continues to be a dynamic and exciting field, with the promise of further advancements that will enhance the efficiency and performance of electric motors across a wide range of applications.

1.4. Challenges

The challenges of the proposed sequential neural network based predictive controller can be stated as follows:

1. Computational complexity: The integration of a sequential neural network with model predictive control requires significant computational power due to the predictive modeling and optimization involved.
2. Data requirements: Accurate training requires high-quality datasets covering diverse motor conditions, which can be challenging to collect and preprocess.
3. Model tuning: Fine-tuning the predictive models to accommodate different load conditions requires careful parameter adjustment and validation.

The proposed MPC model overcomes the challenges and the desired goal with its dynamic modeling and flexible control architecture.

1.5. Contributions

The main contribution of this work is the integration of sequential neural networks (SNN) with model predictive control (MPC) for improved control of permanent magnet synchronous motors (PMSM). The SNN predicts motor behavior, while MPC optimizes real-time adjustments to torque and speed. This hybrid approach ensures smoother and more accurate control compared to genetic

algorithm (GA) and ant colony optimization (ACO) methods. Additionally, it enhances fault detection by learning and recognizing patterns in motor behavior, reducing downtime and improving reliability.

The comparative analysis of the SNN-MPC model against traditional GA and ACO methods has been conducted using a detailed experimental setup that utilized MATLAB and Google Colab's Python environment. This setup allowed for the simulation of PMSM control scenarios, providing a platform for evaluating the performance of each control algorithm. The criteria for performance evaluation included efficiency, response time, and the accuracy of the motor in achieving desired states, such as specific speeds or torque levels and minimum current errors. The experimental analysis revealed that the SNN-MPC model exhibited superior performance in several key areas compared to the GA and ACO methods. Notably, the SNN-MPC model demonstrated enhanced efficiency and faster response times, indicating its potential to significantly improve PMSM control.

1.6. Organization of the paper

The research article demonstrates the dynamic control aspects of various intelligent computational techniques such as GA, ACO, and SNN-MPC models coordinated with predictive attributes. The study and contributions of the paper portray the adaptive and superior predictive control characteristics of the SNN model with respect to GA and ACO by encapsulating the current, speed, and torque responses of the modelled PMSM drive.

This paper is organized as follows: Section 1 presents the introduction with background, review of the literature, motivations, challenges, and contributions from the authors. Section 2 highlights the dynamic modeling of the PMSM and simplified mathematical model of the three phase inverter circuit. In addition to this, predictive control with FCS approach is also included for further assessment. Section 3 depicts the system architectures of the proposed hybrid controllers, those compounded with predictive and intelligent algorithms. These include GA, ACO, and SNN based predictive controllers with an advanced integral action. Section 4 illustrates the dynamic characteristics of current and torque and speed responses of the PMSM tuned from each of the implemented control techniques with a comparison benchmark. The overall research outcomes and determinations from the applied optimization algorithms are presented in Section 5 as concluding revelations.

2. Proposed optimal control methodology

2.1. Model predictive control technique

The model predictive control (MPC) technique stands out for its precision and adaptability, particularly when applied to the control of permanent magnet synchronous motors (PMSMs).

This technique hinges on the accurate prediction and adjustment of motor currents to achieve optimal performance, leveraging the d-q-0 reference frame for current values. The process begins with the specification of reference current values in the d-q frame, which are provided as external inputs. These reference currents, detailed in the context of their time periods, serve as benchmarks for the system's performance. The core of the MPC strategy involves a meticulous comparison between the reference current values and the actual currents measured from the PMSM model. By

utilizing the rotor angle position, the system can transform the reference values from the d-q frame back into three-phase quantities, enabling a direct comparison. The MATLAB simulation block plays a crucial role in this process, predicting the optimal switching states for the converter to minimize the predefined cost function (*J*), i.e., the error between the reference and measured currents. This predictive capability extends to forecasting the load current for upcoming sampling intervals, taking into account the potential voltage vectors that could influence the system's behavior.

2.2. *Dynamic modeling of PMSM drive*

In the exploration of high-efficiency electric motors, the surface-mounted permanent magnet synchronous motor (PMSM) emerges as a prime candidate due to its high power density capabilities. This study models a PMSM, focusing on its behavior in generating sinusoidal back electromagnetic force (EMF) in the absence of field current, deliberately omitting saturation effects on the rotor frame for simplification, as referenced in the work by Wang et al. [1].

$$\frac{di_d}{dt} = \frac{1}{\mathrm{L_d}}\left(\vartheta_d - (\mathrm{R}.i_d) + (\omega_e.\mathrm{L}_q.i_q)\right) \tag{1}$$

$$\frac{di_q}{dt} = \frac{1}{\mathrm{L_q}}\left(\vartheta_q - \left(\mathrm{R}.i_q\right) - (\omega_e.\mathrm{L}_d.i_d) - (\omega_e.\varphi_{mg})\right) \tag{2}$$

$$\frac{d\omega_e}{dt} = \frac{\mathrm{P}}{\mathrm{J}}\left(T_e - \left(\frac{\mathrm{B}}{\mathrm{P}}\omega_e\right) - (T_L)\right) \tag{3}$$

$$T_e = \frac{3}{2}\mathrm{P}\left(i_q.\varphi_{mg} + \left(\mathrm{L}_d - \mathrm{L}_q\right)i_d i_q\right) \tag{4}$$

i_d and i_q are the measured currents in the d-axis and q-axis, expressed in amperes (A). v_d and v_q are the measured voltages in the d-axis and q-axis, expressed in volts (V). ω_s and ω_e are the angular speeds of the stator and rotor, expressed in rad/sec, and φ_{mg} = flux linkage due to permanent magnet (Wb).

The dynamic performance of the PMSM is captured through a set of differential equations that describe the evolution of the d-axis and q-axis currents (Eqs 1 and 2), the rotor's angular speed (Eq 3), and the electromagnetic torque (Eq 4), under the assumption of sinusoidal back EMF and ignoring field current saturation.

The model's foundation rests on the assumption of equal inductance in the d-axis and q-axis ($L_d = L_q$), a characteristic feature of surface-mounted PMSMs, which simplifies the electromagnetic torque equation to Eq 5 when $i_d = 0$. This simplification underscores the model's focus on the direct control of torque through the manipulation of q-axis current, i_q, and the rotor flux constant, φ_{mg}, without the need for d-axis current manipulation. The parameters essential for simulating the PMSM's behavior, including stator resistance, inductance, rotor flux constant, moment of inertia, friction viscous gain, and the number of poles, are meticulously detailed in Table 1, providing a comprehensive overview for replication and further study.

The electromagnetic torque can be expressed as below, with the condition of $i_d = 0$ or surface mounted PMSM with equal inductances, i.e., $\mathrm{L}_d = \mathrm{L}_q$,

$$T_e = \frac{3}{2}\mathrm{P}\left(i_q.\varphi_{mg}\right) \tag{5}$$

Table 1. PMSM parameters [1].

Parameters	Values	Unit
Stator resistance (R)	2.98	Ω
Inductance in d-axis (L_d)	0.007	H
Inductance in q-axis (L_q)	0.007	H
Flux linkage (φ_{mg})	0.125	Wb
Moment of inertia (J)	0.01e-3	Kg·m^2
Friction viscous gain (B)	11e-5	Nm·s
Number of pole pairs (P)	2	

2.3. *Modelling of three phase voltage source inverter*

We consider a 3-φ inverter, which converts 300 V DC to 3-φ AC, for an induction motor of squirrel cage type, whose physical parameters are mentioned in Table 1. The inverter operation having 180° mode of conduction presents a non-linear discrete time system with 7 voltage outputs & 8 configuration states. For simplicity and rounding off, in the modeling and mathematical calculation for the simulation, we ignore the IGBT (Insulated Gate Bipolar Transistor) saturation voltage and diode forward voltage drop. The schematic power circuit of voltage source inverter fed PMSM drive is given below in Figure 1.

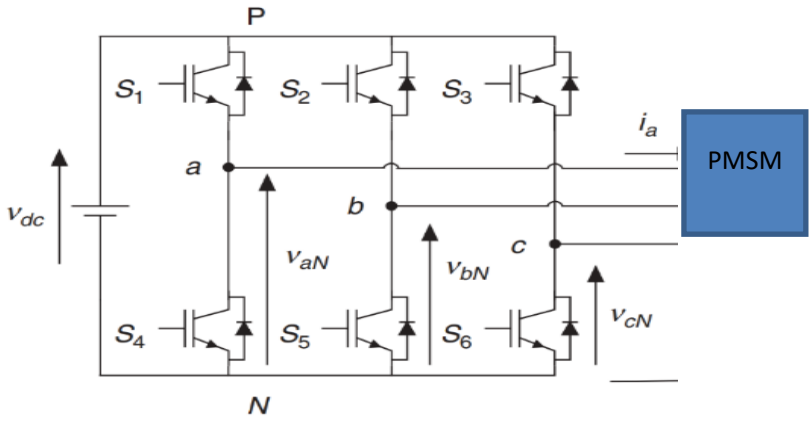

Figure 1. VSI fed PMSM drive.

The switching state for conversions is carried out with the reference of the gating signal, $S_a, S_b,$ and S_c, and represented as follows [1]:

$$S_a = \begin{cases} 1, if\ Switch_1\ on\ and\ Switch_4\ off \\ 0, if\ Switch_1\ off\ and\ Switch_4\ on \end{cases}$$

$$S_b = \begin{cases} 1, if\ Switch_2\ on\ and\ Switch_5\ off \\ 0, if\ Switch_2\ off\ and\ Switch_5\ on \end{cases}$$

$$S_c = \begin{cases} 1, if\ Switch_3\ on\ and\ Switch_6\ off \\ 0, if\ Switch_3\ off\ and\ Switch_6\ on \end{cases}$$

Figure 2 represents the simple mathematical model of the three-phase inverter circuit which shows the output voltage generation by means of switching signal application. These switching states are generated by the optimum operation of predictive algorithms. The details of controlled state evaluation by the proposed controllers are described in the next section

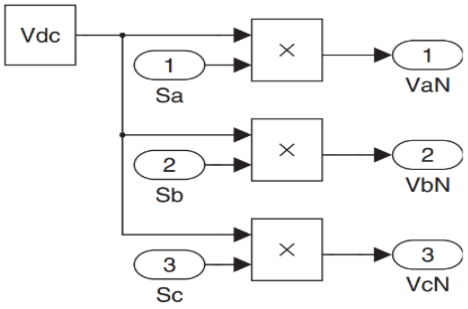

Figure 2. Voltage output of VSI.

2.4. Calibration of MPC with finite control set (FCS)

The calibration of model predictive control (MPC) with a finite control set (FCS) was undertaken to enhance the control of permanent magnet synchronous motors (PMSM), integrating the predictive prowess of MPC with the discrete operational framework of FCS. This method optimized the switching states of the power converter, aiming for precise and efficient motor performance. In this approach, the control action was selected from a finite set of possible inverter switching states, directly addressing the discrete nature of power converters and negating the need for additional modulation processes. The calibration process entailed the development of a predictive motor model that accurately reflected the motor's dynamics under various switching states and the formulation of a cost function to quantify deviations from desired performance metrics. The MPC algorithm evaluated each possible switching state's impact on future motor behavior, selecting the one that minimized the cost function. This selection process, repeated at each control interval, allowed for real-time adjustments to motor operation or load changes. The calibration of FCS-MPC also involved tuning the prediction horizon and cost function weighting factors, balancing control objectives with computational limitations, thereby ensuring the scheme's effective real-time operation. The space vector modulation (SVM) scheme [17], a refined method, is used here to regulate the output voltage by controlling the optimal switching states. This approach allowed for precise control of the amplitude and phase of the inverter's output voltage, enabling efficient and smooth operation of AC motors such as the PMSM.

The generation of switching states gives rise to eight voltage vectors, provided in Table 3, which can be predicted by Equation (6) as follows [1,3,9]:

$$v = \frac{2}{3} V_{dc} (S_a + aS_b + a^2 S_c) \tag{6}$$

Table 2. Switching states with voltage vectors [17].

S_a	S_b	S_c	Voltage vector ($\vec{v}$)	
0	0	0	$\overrightarrow{v_0} = 0$	
1	0	0	$\overrightarrow{v_1} = \frac{2}{3} v_{dc}$	
1	1	0	$\overrightarrow{v_2} = \frac{1}{3} v_{dc} + j \frac{\sqrt{3}}{3} v_{dc}$	where
0	1	0	$\overrightarrow{v_3} = -\frac{1}{3} v_{dc} + j \frac{\sqrt{3}}{3} v_{dc}$	a = $e^{-j(2\pi/3)} = -\frac{1}{2} + j\frac{\sqrt{3}}{2}$, with a phase displacement of 120 ° between any two phases in Equation (6)
0	1	1	$\overrightarrow{v_4} = -\frac{2}{3} v_{dc}$	
0	0	1	$\overrightarrow{v_5} = -\frac{1}{3} v_{dc} - j \frac{\sqrt{3}}{3} v_{dc}$	
1	0	1	$\overrightarrow{v_6} = \frac{1}{3} v_{dc} - j \frac{\sqrt{3}}{3} v_{dc}$	
1	1	1	$\overrightarrow{v_7} = 0$	

The generalized equations for the predicted load current in the direct-quadrature (d-q) frame using forward Euler approximations, which are methods for numerically integrating differential equations, are defined in Eqs (7) and (8), respectively [1,4,9].

$$\frac{di_d(t)}{dt} \approx \frac{i_d(t_{i+1}) - i_d(t_i)}{T_s} \tag{7}$$

$$\frac{di_q(t)}{dt} \approx \frac{i_q(t_{i+1}) - i_q(t_i)}{T_s} \tag{8}$$

$$i_d(t_{i+1}) = i_d(t_i) + \frac{T_s}{L_d}(v_d(t_i) - Ri_d(t_i) + \omega_e(t_i) L_q i_q(t_i)) \tag{9}$$

$$i_q(t_{i+1}) = i_q(t_i) + \frac{T_s}{L_q}(v_q(t_i) - Ri_q(t_i) + \omega_e(t_i) L_d i_d(t_i)) - \omega_e(t_i)\varphi_{mg}) \tag{10}$$

Equations (7) and (8) approximated the rate of change of the direct axis current, i_d, and the quadrature axis current, i_q, respectively. The subsequent equations, (9) and (10), provided the predicted load currents for the next time interval, t_{i+1}, by incorporating the voltage across the PMSM input terminals.

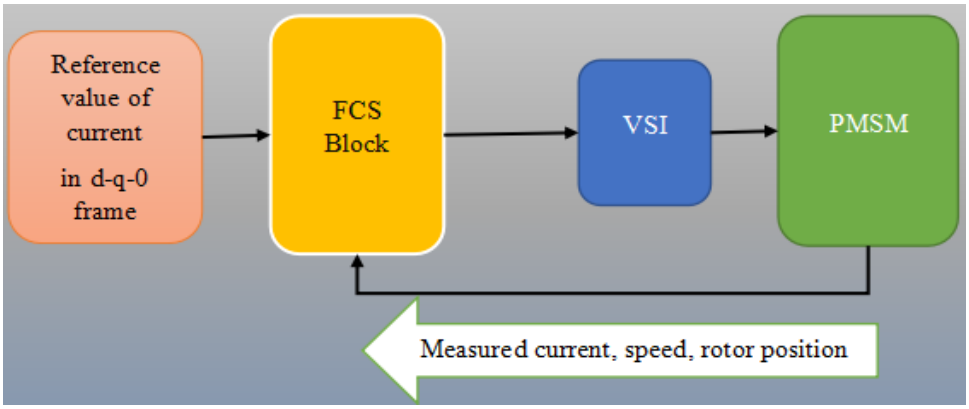

Figure 3. Structure of FCS-MPC method in d-q coordinates.

Figure 5 depicts a control system for a permanent magnet synchronous motor (PMSM) where the system began with the generation of a reference current value in the direct-quadrature (d-q) frame, which was then fed into the field-oriented control (FOC) system (FCS) block. This block was responsible for determining the appropriate control signals to achieve the desired motor performance by aligning the stator and rotor fields. The output from the FCS block was directed to a voltage source inverter (VSI), which converted the DC power into AC power with the necessary amplitude and frequency to drive the PMSM. The performance of the motor was continuously monitored by measuring the current, speed, and rotor position. These measurements were fed back into the FCS block, creating a closed-loop control system that dynamically adjusted the reference values to meet the desired performance criteria. This control methodology allowed for precise speed and torque control of the PMSM, which was essential for applications requiring high efficiency and dynamic response.

In this study a two-level, three-phase VSI is considered for application of predictive schemes. As the overall modelling and computations are in the d-q-0 reference frame, the voltage vectors generated need to be transformed to d-q-0 coordinates from a-b-c coordinates by means of Park's transformation.

$$\begin{bmatrix} \vartheta_d \\ \vartheta_q \end{bmatrix} = \frac{2}{3}\begin{bmatrix} cos\theta & \cos(\theta - \frac{2\pi}{3}) & \cos(\theta + \frac{2\pi}{3}) \\ -sin\theta & -\sin(\theta - \frac{2\pi}{3}) & -\sin(\theta + \frac{2\pi}{3}) \end{bmatrix}\begin{bmatrix} V_{an} \\ V_{bn} \\ V_{cn} \end{bmatrix} \tag{11}$$

where ϑ_d = voltage in d-axis, ϑ_q = voltage in q-axis, and θ = rotor position angle. V_{an}, V_{bn}, and V_{cn} are the phase voltages of a-b-c with respect to neutral, respectively, and V_{dc} = DC voltage supplied to VSI.

The switching combinations and corresponding voltage vectors imposed in the FCS-MPC technique are shown in Table 3.

Table 3. Switching states with voltage vectors [17].

S_a	S_b	S_c	Voltage vector ($\vec{v}$)	V_{an}	V_{bn}	V_{cn}
0	0	0	$\overrightarrow{v_0}$	$-\frac{V_{dc}}{2}$	$-\frac{V_{dc}}{2}$	$-\frac{V_{dc}}{2}$
1	0	0	$\overrightarrow{v_1}$	$\frac{V_{dc}}{2}$	$-\frac{V_{dc}}{2}$	$-\frac{V_{dc}}{2}$
1	1	0	$\overrightarrow{v_2}$	$\frac{V_{dc}}{2}$	$\frac{V_{dc}}{2}$	$-\frac{V_{dc}}{2}$
0	1	0	$\overrightarrow{v_3}$	$-\frac{V_{dc}}{2}$	$\frac{V_{dc}}{2}$	$\frac{V_{dc}}{2}$
0	1	1	$\overrightarrow{v_4}$	$-\frac{V_{dc}}{2}$	$\frac{V_{dc}}{2}$	$\frac{V_{dc}}{2}$
0	0	1	$\overrightarrow{v_5}$	$-\frac{V_{dc}}{2}$	$-\frac{V_{dc}}{2}$	$\frac{V_{dc}}{2}$
1	0	1	$\overrightarrow{v_6}$	$\frac{V_{dc}}{2}$	$-\frac{V_{dc}}{2}$	$\frac{V_{dc}}{2}$
1	1	1	$\overrightarrow{v_7}$	$\frac{V_{dc}}{2}$	$\frac{V_{dc}}{2}$	$\frac{V_{dc}}{2}$

where $\begin{bmatrix} V_{an} \\ V_{bn} \\ V_{cn} \end{bmatrix} = \begin{bmatrix} S_a - \frac{1}{2} \\ S_b - \frac{1}{2} \\ S_c - \frac{1}{2} \end{bmatrix} V_{dc}$

In the FCS-MPC approach, there are seven sets of v_d and v_q values are presented based on the rotor angular position and sampling time. In this control strategy, the objective function is defined as the sum of the squares of the errors between the desired and predicted current values in the d-q frame. The objective function (J) is

$$J_K = \{i_d{}^*(\mathrm{t_i}) - i_d(t_{i+1})\}^2 + \{i_q{}^*(\mathrm{t_i}) - i_q(t_{i+1})\}^2 \quad (12)$$

where $i_d(t_{i+1})$ and $i_q(t_{i+1})$ are the predicted values of current in the d-q frame, $i_d{}^*$and $i_q{}^*$ are the desired values of current in the d-q frame, respectively, and $\mathrm{t_i}$ is the sampling instant. By combining Eqs (9) and (10), Equation (12) can be further modified as

$$J_k = \left(i_d^*(t_i) - i_d(t_i) - \frac{T_s}{L_d}\left(v_d(t_i) - Ri_d(t_i) + \omega_e(t_i)L_q i_q(t_i)\right)\right)^2 + \left(i_q^*(t_i) - i_q(t_i) - \frac{T_s}{L_q}\left(v_q(t_i) - Ri_q(t_i) - \omega_e(t_i)L_d i_d(t_i) - \omega_e(t_i)\varphi_{mg}\right)\right)^2 \quad (13)$$

where φ_{mg} = rotor flux constant or flux linkage, and k is the index from 0 to 7.

The control system utilized a receding horizon principle, which predicts the next step's values based on the current feedback parameters such as the direct and quadrature currents $i_d(t_i)$ and $i_q(t_i)$, the electrical angular velocity ω_e, and the electrical angle θ_e, from the PMSM model. The objective function was computed for each pair of v_d–v_q values using these feedback parameters from the PMSM model, and the one that minimized this function was selected for the next control action. Additionally, for programming convenience, the equations governing the system's dynamics were also represented in matrix form as follows:

$$\begin{bmatrix} i_d(t_{i+1}) \\ i_q(t_{i+1}) \end{bmatrix} = (\mathrm{I}+T_s A_m(t_i)) \begin{bmatrix} i_d(t_i) \\ i_q(t_i) \end{bmatrix} + T_s B_m \begin{bmatrix} v_d(t_i) \\ v_q(t_i) \end{bmatrix} - \begin{bmatrix} 0 \\ \dfrac{\omega_e(t_i)\varphi_{mg} T_s}{L_q} \end{bmatrix} \tag{14}$$

where I is the identity matrix of dimension 2×2

$$A_m(t_i) = \begin{bmatrix} \dfrac{-R_s}{L_d} & \dfrac{w_e(t_i)L_q}{L_d} \\ \dfrac{-w_e(t_i)L_d}{L_q} & \dfrac{-R_s}{L_q} \end{bmatrix} \tag{15}$$

$$B_m = \begin{bmatrix} \dfrac{1}{L_d} & 0 \\ 0 & \dfrac{1}{L_q} \end{bmatrix} \tag{16}$$

Equation (14) expressed the predicted current values as a function of the voltages, current, and inductances in the d-q frame, flux linkage, electrical velocity, and sampling time. Matrix $A_m(t_i)$ and B_m are derived from Eqs (9) and (10) and expressed in Eqs (15) and (16), respectively. This formulation provided a clear framework for developing the control algorithms that would operate the PMSM efficiently, ensuring optimal performance in accordance with the control objectives.

From the optimal output feedback control framework in the FCS-MPC method, it can be obtained that

$$\begin{bmatrix} v_d(t_i)^{opt} \\ v_q(t_i)^{opt} \end{bmatrix} = K_{fcs} \left(\begin{bmatrix} {i_d}^*(t_i) \\ {i_q}^*(t_i) \end{bmatrix} - \begin{bmatrix} i_d(t_i) \\ i_q(t_i) \end{bmatrix} \right) \tag{17}$$

where K_{fcs} is the gain of the optimal voltage matrix.

3. Proposed predictive controller for integration with intelligent computational algorithms

The FCS-MPC system has one major disadvantage of a unit time delay when a closed loop value is approximated. So, the FCS-MPC system contains some steady stable error due to the closed loop action [2,11,12]. The best method to eliminate steady state error is integral action on an outer-loop controller. Since the system states are continuous in nature, sampling the response of the system by the FCS-MPC method creates a poor inter-sample response. This can be avoided by taking an integral term of error between desired and predicted values in the cost function. The algorithm used here operates on reference values and measured values in the d-q frame. Speed and rotor angular position are also used for providing switching states to the inverter. Except the steady state error, the integral action also improves the rejecting quality of low frequency disturbance. Hence, the mathematical definition of the optimal voltages obtained from the integral finite control set (IFCS) predictive controller in the discrete time control system can be modified as follows:

$$\begin{bmatrix} v_d(t_i)^{opt} \\ v_q(t_i)^{opt} \end{bmatrix} = K_{fcs} \begin{bmatrix} \frac{K_d}{1-q^{-1}} \left(i_d{}^*(t_i) - i_d(t_i)\right) \\ \frac{K_q}{1-q^{-1}} \left(i_q{}^*(t_i) - i_q(t_i)\right) \end{bmatrix} - K_{fcs} \begin{bmatrix} i_d(t_i) \\ i_q(t_i) \end{bmatrix} \tag{18}$$

where K_d and K_q are the values of integral block parameters used for current error at both the d-axis and q-axis, respectively, $0 < K_d \leq 1$, and $0 < K_q \leq 1$. $\frac{1}{1-q^{-1}}$ represents functionality of an integrator.

The structure of IFCS-MPC is depicted below in Figure 4. In the proposed IFCS predictive controller, the inner loop presents the FCS control, and the outer loop demonstrates the integral action of the controller.

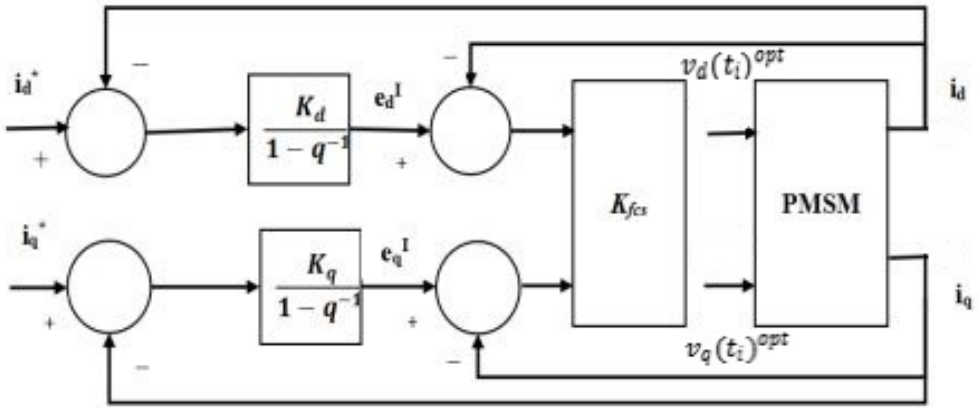

Figure 4. Structure of IFCS-MPC method.

The objective function, J_k is calculated for seven pairs of candidate variables for v_d and v_q voltages. The objective function is calculated for k = 0, 1, 2, 6.

$$J_K = \frac{T_s{}^2}{L_d{}^2} \left(v_d(t_i)^K - v_d(t_i)^{opt}\right)^2 + \frac{T_s{}^2}{L_q{}^2} \left(v_q(t_i)^K - v_q(t_i)^{opt}\right)^2 \tag{19}$$

where $T_s =$ sampling interval, and L_d, L_q are d-axis and q-axis inductance, respectively.

The matrix representation of newly defined equation of d-q currents that shows the integral action of MPC is presented in Eq (20).

$$\begin{bmatrix} i_d(t_{i+1}) \\ i_q(t_{i+1}) \end{bmatrix} = (\mathrm{I} + T_s A_m(t_i) - T_s B_m K_{fcs}) \begin{bmatrix} i_d(t_i) \\ i_q(t_i) \end{bmatrix} + T_s B_m K_{fcs} \begin{bmatrix} e_d(t_i)^I \\ e_q(t_i)^I \end{bmatrix} - \begin{bmatrix} 0 \\ \frac{\omega_e(t_i)\varphi_{mg}\,\Delta t}{L_q} \end{bmatrix} \tag{20}$$

where I is the identity matrix of (2×2),

$$A_m(t_i) = \begin{bmatrix} \frac{-R_s}{L_d} & \frac{w_e(t_i)L_q}{L_d} \\ \frac{-w_e(t_i)L_d}{L_q} & \frac{-R_s}{L_q} \end{bmatrix} \tag{21}$$

$$B_m = \begin{bmatrix} \frac{1}{L_d} & 0 \\ 0 & \frac{1}{L_q} \end{bmatrix} \tag{22}$$

φ_{mg} = Flux magnitude in webers,
$e_d{}^I$ and $e_q{}^I$ are integral errors of d-axis and q-axis, respectively.

The applied intelligent predictive computational techniques are scheduled by the optimized criteria defined in Eqs (18) and (19) to diagnose their superiorities in terms of optimized gains, current, torque, and speed responses of the modeled PMSM.

3.1. Sequential neural network on PMSM

The sequential neural network (SNN) on a permanent magnet synchronous motor (PMSM) represents a sophisticated approach in motor control technology. Leveraging the sequential processing capabilities of neural networks, the SNN architecture is designed to sequentially process input data, such as motor currents and rotor positions, to dynamically control the PMSM. By learning from the temporal patterns of the motor's behavior, the SNN can make informed predictions and adjustments to the control signals, ensuring optimal motor performance.

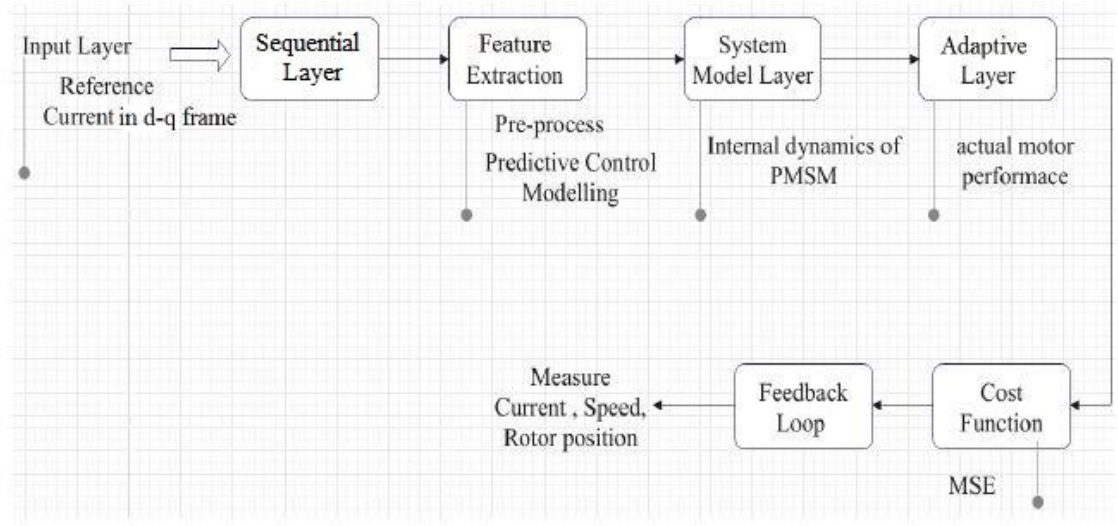

Figure 5. Proposed sequential network for PMSM.

Figure 6 structure outlines the design of a sequential neural network (SNN) tailored for controlling a permanent magnet synchronous motor (PMSM). Commencing with the input layer block, the network receives the reference current in the d-q-0 frame and potentially other motor parameters. Next, the pre-processing block prepares the input data for further analysis, akin to signal conditioning. Subsequently, the feature extraction block processes the data to discern pivotal characteristics essential for motor control.

The PMSM dynamics block functions as a virtual model of the motor, capturing its intrinsic dynamic behavior. An adaptive parameter tuning block is responsible for refining the network's

parameters in real time, ensuring the model's accuracy as operating conditions change. The control decision block then determines the optimal control actions required. The cost function evaluation block measures the performance of these actions against a predefined cost function, typically involving the minimization of error between desired and actual motor performance. The output layer block generates the final control signals to the motor's inverter. Finally, a feedback loop block, crucial during the training phase, allows the network to learn from the system's actual performance and continuously adjust its predictions, embodying a dynamic learning capability essential for real-world applications. The sequential search parameters for the proposed neural network are selected as follows.

I. Search range: [-1, 1] for both i_d and i_q
II. Resolution: 100×100 grid points
III. Iterations: Implicit in the resolution, totaling 1000

The proposed method emphasizes computational efficiency through optimized predictive algorithms and intelligent data processing. The computational complexity, due to the sequential neural network processing, is mitigated by model optimization and reducing unnecessary data paths. The runtime remains practical for real-world applications due to the model's efficient MPC integration and the SNN's predictive learning. We discuss computational complexity in detail, noting that the optimized model provides practical predictive accuracy while maintaining acceptable runtimes.

3.2. Genetic algorithm for PMSM

The application of a genetic algorithm (GA) to a permanent magnet synchronous motor (PMSM) involves using this evolutionary computational technique to optimize the motor's performance parameters. In this context, a GA starts by randomly initializing a population of potential solutions, each representing a set of PMSM control parameters. These individuals are then evaluated for their fitness, which reflects how well they meet the predefined performance criteria, such as efficiency, torque ripple, or speed control.

The GA iteratively improves the population through genetic operations—selection, crossover, and mutation—based on the fitness values. Over successive generations, the GA converges towards optimal solutions, satisfying termination conditions such as a maximum number of iterations or a satisfactory fitness level. The result is a set of optimized control parameters that enhance the PMSM's operation, potentially leading to improvements in energy consumption, dynamic response, and overall system robustness.

The flowchart in Figure 6 illustrates a genetic algorithm (GA) process used for optimization tasks. The process starts with the random initialization of a population of potential solutions, denoted as population N. Each individual solution within this population is evaluated for its fitness, indicated by the function Ef(x), which determines how well it solves the optimization problem or fits the desired criteria. Subsequently, a cost evaluation is performed for each solution based on the same fitness values, which could be indicative of an additional evaluation metric or a penalty function integrated into the optimization process.

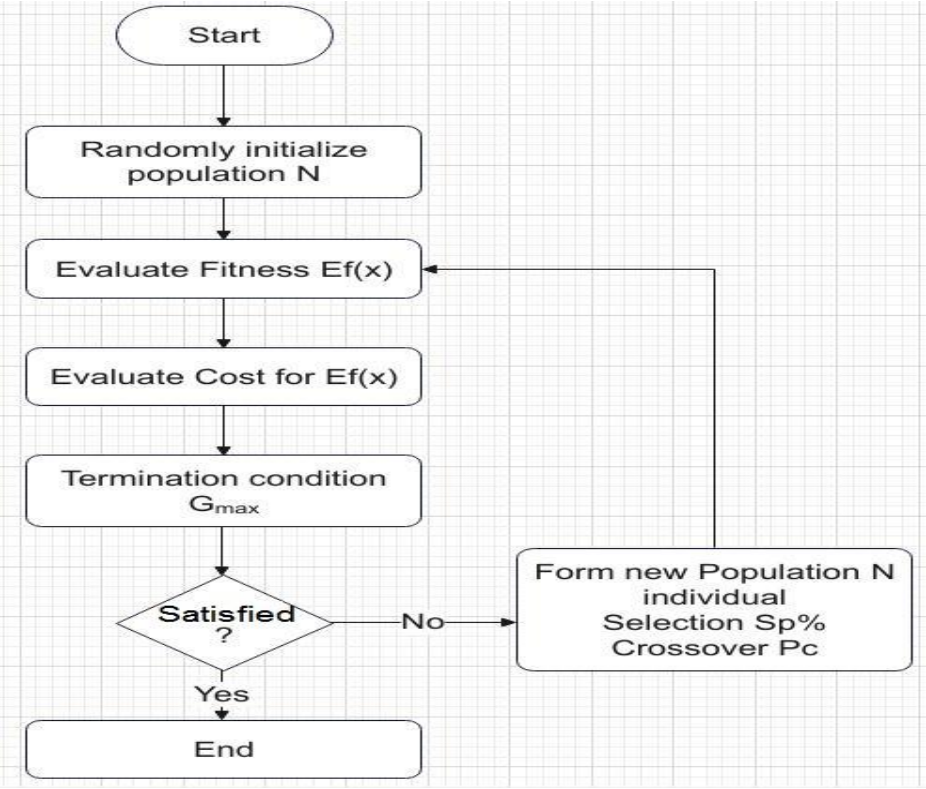

Figure 6. Flowchart of GA for PMSM.

As the algorithm proceeds, it continually checks against a termination condition, typically defined by a maximum number of generations, G_{max}. If this condition is not met, the algorithm is not satisfied, and it goes on to form a new population. This new generation of solutions is created using genetic operators such as selection (with a probability Sp%) and crossover (with a probability Pc). These operators are fundamental to GA, as they combine and modify solutions in search of improved fitness and cost evaluations. The loop continues until the termination condition is satisfied, at which point the process ends, hopefully having identified a near-optimal solution to the problem at hand.

3.3. Ant colony optimization for PMSM

Ant colony optimization (ACO) applied to a permanent magnet synchronous motor (PMSM) leverages the bio-inspired algorithm to find optimal pathways for parameter adjustment and control in the motor's management system. The ACO mimics the foraging behavior of ants to solve complex optimization problems. In the context of PMSM, a colony of artificial ants systematically searches through the multi-dimensional space of motor parameters, such as voltage levels, current profiles, and timing of phase commutations. These ants lay down pheromones on paths that yield better motor performance, with the pheromone intensity guiding subsequent searches towards these promising areas. Over time, the artificial ants converge on a set of solutions that optimize PMSM operation for criteria like minimizing energy consumption, maximizing efficiency, or achieving precise speed and torque control. This approach is particularly beneficial for PMSMs due to their nonlinear characteristics and the complex interplay of their control variables. Through ACO, engineers can derive control strategies that enhance the PMSM's functionality in various applications, from electric vehicles to industrial automation systems.

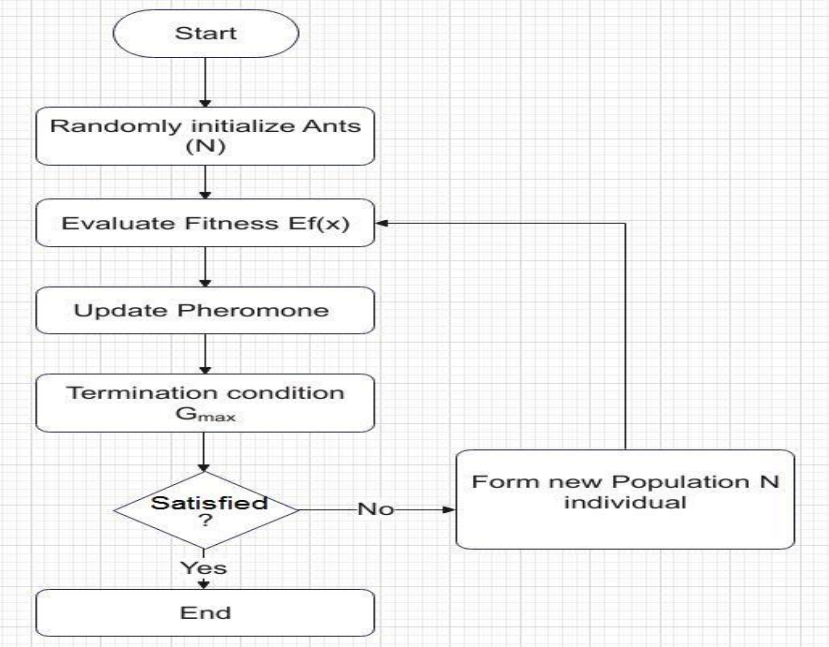

Figure 7. Flowchart of ACO for PMSM.

The flowchart shown in Figure 7 illustrates the steps of an ant colony optimization (ACO) algorithm adapted for optimizing control parameters in a permanent magnet synchronous motor (PMSM). The process begins with the initialization of a number of ants, each representing a potential solution. These ants explore the solution space by evaluating the fitness values of their positions with respect to the control problem, akin to assessing how well a set of PMSM parameters performs a given task. Based on the fitness evaluation, the ants then update the pheromone levels on their paths, effectively communicating the quality of their solutions to guide subsequent search efforts.

The algorithm iterates over this process, continuously updating pheromones and steering the colony towards more promising areas of the solution space. The iteration continues until a termination condition, typically a predefined number of cycles or a satisfactory level of solution quality, is met. If the condition is not met, a new generation of solutions is formed, influenced by the accumulated pheromones. Once the termination criterion is satisfied, indicating that an optimal or near-optimal solution has likely been found, the process ends. This approach enables a collective, pheromone-guided search strategy that is effective for finding optimal control strategies in complex systems like PMSMs. The parameters selected for the optimization process of GA and ACO are mentioned in Table 4.

Table 4. Parameter constraints used for GA and ACO.

GA Parameters	ACO Parameters
Population size = 500	Number of Ants = 500
Generations = 100	Iterations = 1000
Crossover probability (cxpb) = 0.5	Pheromone evaporation rate = 0.5 per iteration
Mutation probability (mutb) = 0.2	Pheromone deposit rate: conceptual rate = 0.1
Mutation: Gaussian, mu, $\mu = 0$, sigma, $\sigma = 0.2$, indpb = 0.1	Search space: [-1,1] for both i_d and i_q
Selection: Tournament, toursize = 3	

4. Results and analysis

Investigating advanced control algorithms for a three-phase induction motor, we introduced a novel control model named SNN-MPC, a sequential neural network model predictive control algorithm, which was meticulously developed and tested. Subsequently, this innovative approach was subjected to a comparative analysis alongside two other established algorithms: genetic algorithm (GA) and ant colony optimization (ACO). The comparative study was rigorously designed to assess the dynamic responses of the induction motor, with a keen focus on the currents, torque, and angular speed, under the governance of these predictive control schemes. Each algorithm was applied to the motor's inverter circuit, and simulations were conducted to ensure a robust evaluation of their performances.

The simulation parameters were standardized across all models to ensure a fair comparison, maintaining a total simulation time of 0.2 seconds with a sampling interval of 10 microseconds. The SNN-MPC model's performance metrics were benchmarked against those achieved by the GA and ACO methods, which represent the current state-of-the-art in predictive control algorithms. This comparative analysis is critical to determining the efficacy of the SNN-MPC model in enhancing motor control dynamics. The forthcoming results and discussions aim to illuminate the strengths and potential areas of improvement for each algorithm, providing a comprehensive overview without deviation from the original simulation terms set forth in the experimental setup.

4.1. Experimental setup

In the experimental setup for the comparative analysis of control algorithms on a three-phase induction motor, both MATLAB and Google Colab's Python environment were utilized as the primary computational tools. MATLAB, known for its robust toolbox for simulation and model-based design, was employed for its advanced capabilities in handling and modeling complex control systems like SNN-MPC, GA, and ACO algorithms. Complementing this, Google Colab offered a versatile Python environment with powerful libraries for machine learning and numerical computation, enabling the implementation and testing of the proposed sequential neural network model predictive control (SNN-MPC) algorithm. The integration of these two platforms provided a comprehensive approach to the simulation tasks, allowing for extensive data analysis and algorithm optimization. In the context of the PMSM dynamics analysis step input reference currents in the d-q frame and also a step signal of input load torque have been applied to the modeled machine drive. These signals insist to continue through the predicted output trajectories.

4.2. Experimental results

4.2.1. Optimized gain parameters (K_d, K_q, K_{fcs})

The fine-tuning of the controller parameters, specifically the direct-axis gain (K_d), the quadrature gain (K_q), and the feedback control gain (K_{fcs}), for the PMSM is crucial to achieve a precise and stable control of the motor's speed and torque. K_d was adjusted to optimize the system's response to changes in error rate, enhancing the motor's dynamic behavior. K_q, on the other hand, was fine-tuned to regulate the quadrature-axis current component, directly influencing torque production.

Table 5. Optimized gain parameters

Tuning Technique	K_d	K_q	K_{fcs}
SNN	0.01	0.006	0.13
GA	0.09	0.0056	0.19356
ACO	0.098	0.007824	0.18236

The table outlines the optimized gain parameters' values obtained from different tuning techniques applied to control systems, specifically using the sequential neural network (SNN), genetic algorithm (GA), and ant colony optimization (ACO) methods. For the SNN, the tuning resulted in a d-axis gain (K_d) of 0.01, a quadrature gain (K_q) of 0.006, and a feedback gain of inner loop in the IFCS architecture (K_{fcs}) of 0.13, indicating a balanced approach to responsiveness and stability.

The GA technique, known for its ability to navigate complex optimization landscapes, yielded slightly higher gains: K_d at 0.09, K_q at 0.0056, and K_{fcs} at 0.19356, suggesting a strategy leaning more towards aggressive control to minimize error and optimize performance. Lastly, the ACO method, which simulates the foraging behavior of ants to find optimal solutions, determined K_d to be 0.098, K_q to be 0.007824, and K_{fcs} to be 0.18236. These values reflect a fine-tuned balance, likely aiming to enhance system dynamics while maintaining robustness against disturbances. Each set of parameters reflects the inherent characteristics and optimization strategies of the respective tuning technique, demonstrating the diverse approaches to achieving desired control objectives in complex systems.

4.2.2. Current dynamic analysis

The reference current in the d-q frame for system dynamics analysis is depicted in Figure 8.

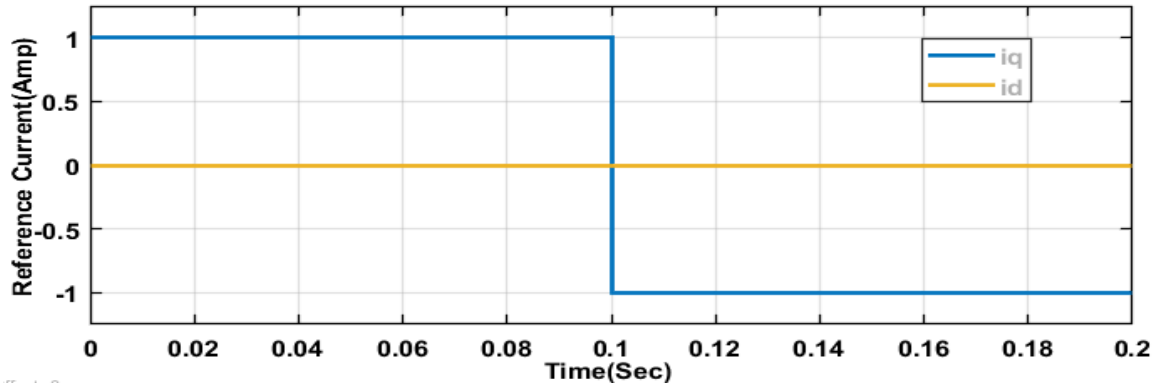

Figure 8. Applied reference currents in d-q frame.

The plots provided in Figure 9 represent the dynamic current responses of a three-phase induction motor under the control of three different optimization algorithms: ant colony optimization (ACO), genetic algorithm (GA), and sequential neural network (SNN) control strategies. In these graphs, the direct-axis current (*id*) and quadrature-axis current (*iq*) are plotted over time, giving insights into the performance characteristics of each control method applied to the motor.

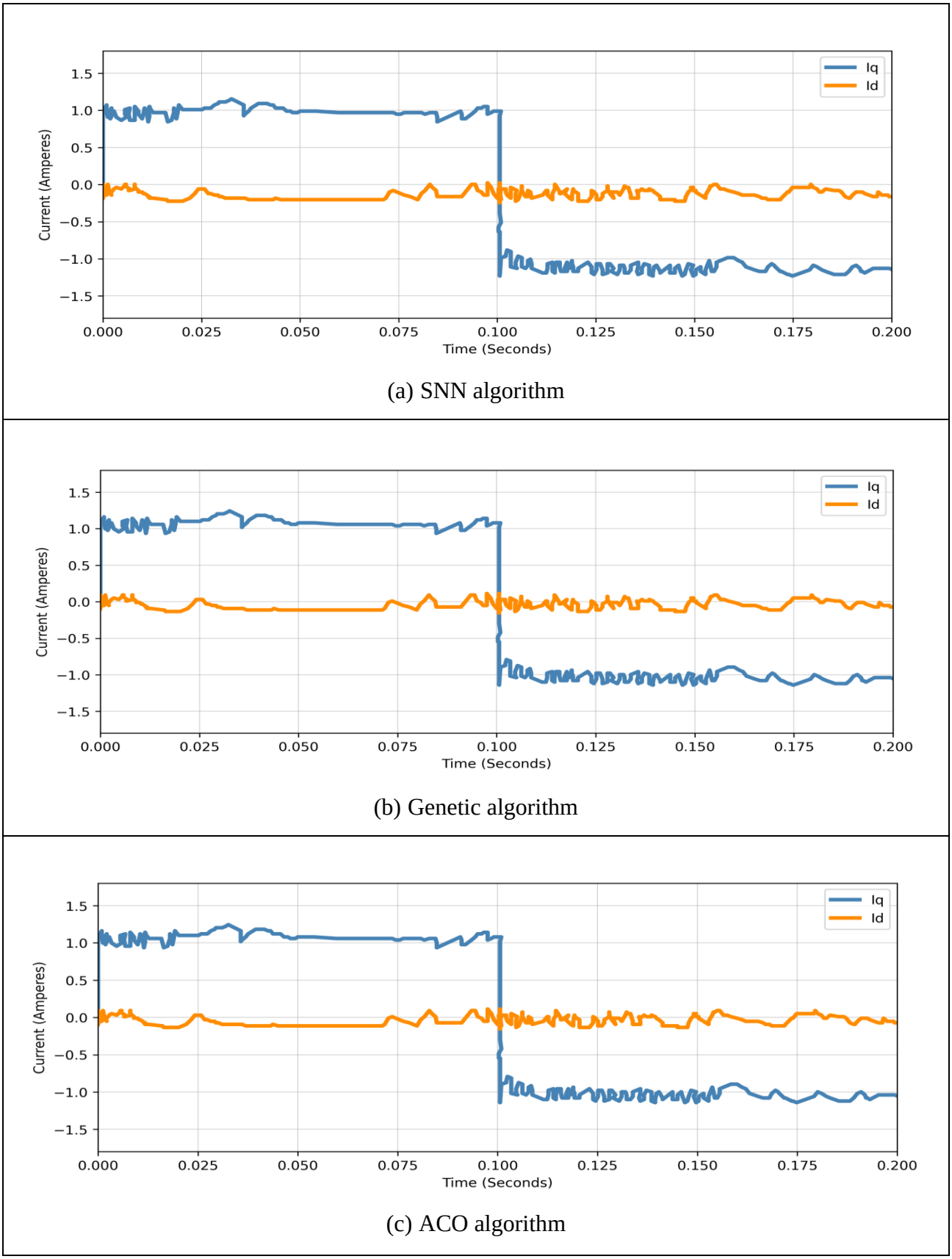

(a) SNN algorithm

(b) Genetic algorithm

(c) ACO algorithm

Figure 9. Results of optimized algorithm in real-time current analysis.

For the ACO algorithm, the quadrature current exhibits a steady-state behavior with minimal fluctuation around the 1.0 ampere mark, while the direct axis current shows a negative spike before stabilizing close to zero, indicating a reactive control action due to a change in load or reference input. The GA plot shows both *id* and *iq* currents presenting with higher variability and a sudden drop, followed by a quick recovery, which might suggest a transient response to a perturbation in the system or a shift in control targets. Both currents then stabilize, with *iq* maintaining a slightly positive value and *id* trending towards a steady negative value, likely indicative of the algorithm's strategy to balance torque production against magnetic flux regulation.

The SNN strategy graph reveals a more consistent and less volatile profile for both iq and id currents, with *iq* hovering just above 1.0 amperes and *id* remaining close to zero throughout the simulation period. This could be interpreted as a more conservative control approach, prioritizing stability and smooth response over aggressive adjustments. Overall, the graphs display the distinctive impacts of each control algorithm on motor currents, reflecting their inherent operational strategies and tuning philosophies. The ACO and GA plots show more aggressive responses to system changes, potentially providing faster adaptability at the cost of higher transient fluctuations. In contrast, the SNN strategy's plot suggests a focus on maintaining steady-state operation with minimal disturbances, potentially at the cost of slower responsiveness to abrupt system changes. Each control method's suitability would therefore depend on the specific performance criteria and application requirements for the motor control system.

4.2.3. Predicted torque trajectories

The provided plots in Figure 10 illustrate the torque response of a permanent magnet synchronous motor (PMSM) over a simulated time span of 0.2 seconds, controlled by three different optimization techniques: ant colony optimization (ACO), genetic algorithm (GA), and sequential neural network (SNN) strategy. Each plot captures the motor's torque as a function of time, shedding light on the effectiveness of the respective control algorithm in managing the PMSM's performance. Figure 10(a) depicts the reference load torque applied to the modeled drive. A step signal (Figure 10(a)) is applied to the PMSM, and the predicted torque outputs are acquired as the electrical torque with respect to the enforced intelligent optimization proficiencies.

In all three scenarios, the torque appears to maintain a relatively steady state initially, hovering around 1 Nm, which suggests a well-balanced system under nominal operating conditions. However, a sharp decline in torque is observed in the latter part of the simulation, indicating a sudden reduction in load or a change in the command signal. The motor's reaction to this change is critical to understanding each control strategy's robustness and adaptability. The ACO-controlled motor shows a stable response before and after the torque dip, implying that the ACO algorithm quickly adapts to changes, stabilizing the motor with minimal oscillation. The GA approach reveals a similar pattern, with the torque returning to a stable state post-disturbance, suggesting the GA's effectiveness in managing the PMSM's dynamics. Lastly, the SNN strategy demonstrates a consistent torque profile, with the system returning to a steady state after the initial disturbance. This consistent response may indicate that the SNN strategy is tuned for a balance between responsiveness and stability, ensuring the motor operates smoothly throughout varying conditions.

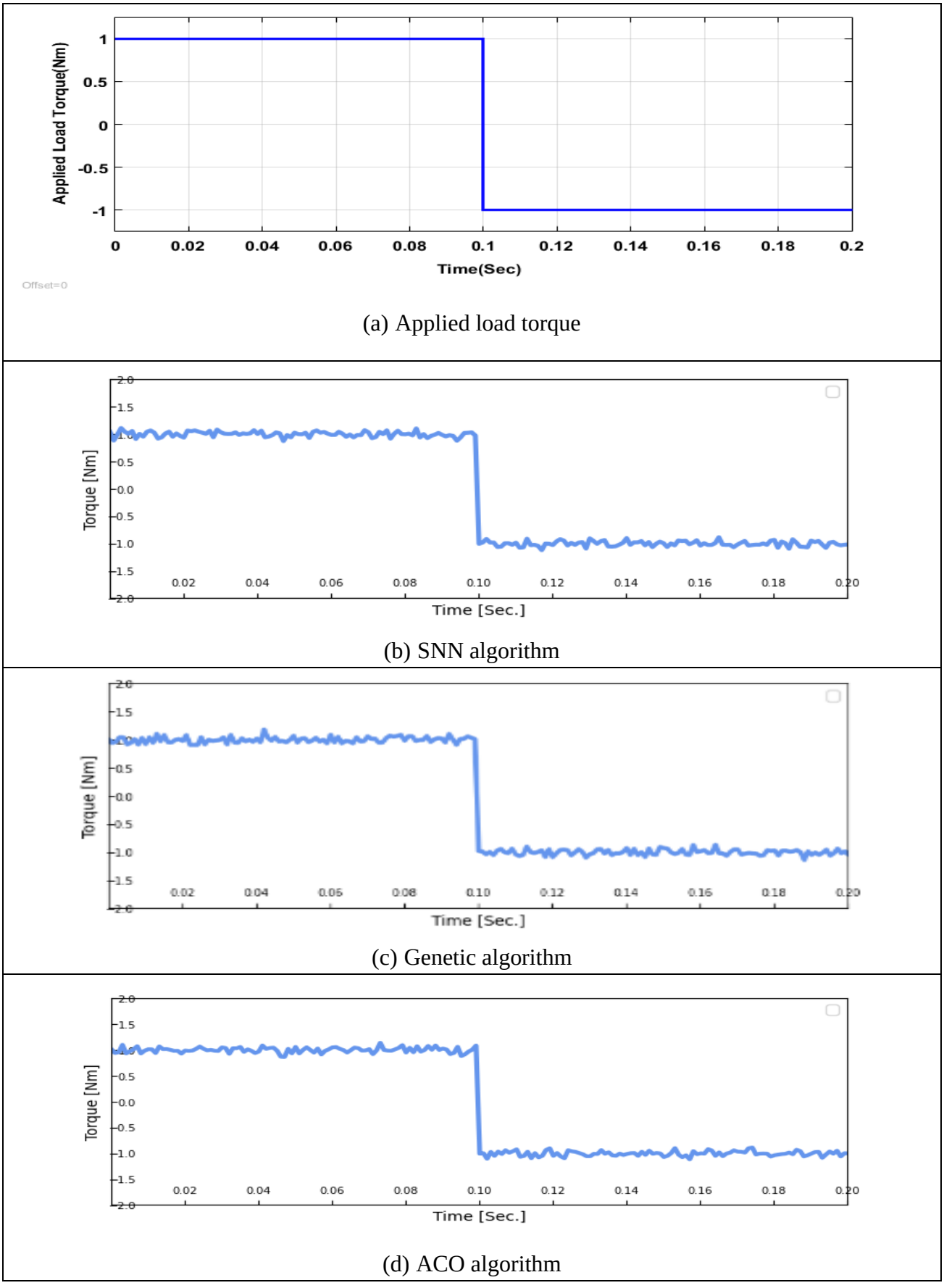

Figure 10. Torque responses of applied optimization algorithms.

4.2.4. Speed and rotor angle characteristics

The speed responses and rotor angle trajectories extracted from each of the scheduled prediction algorithms have been illustrated in Figure 11.

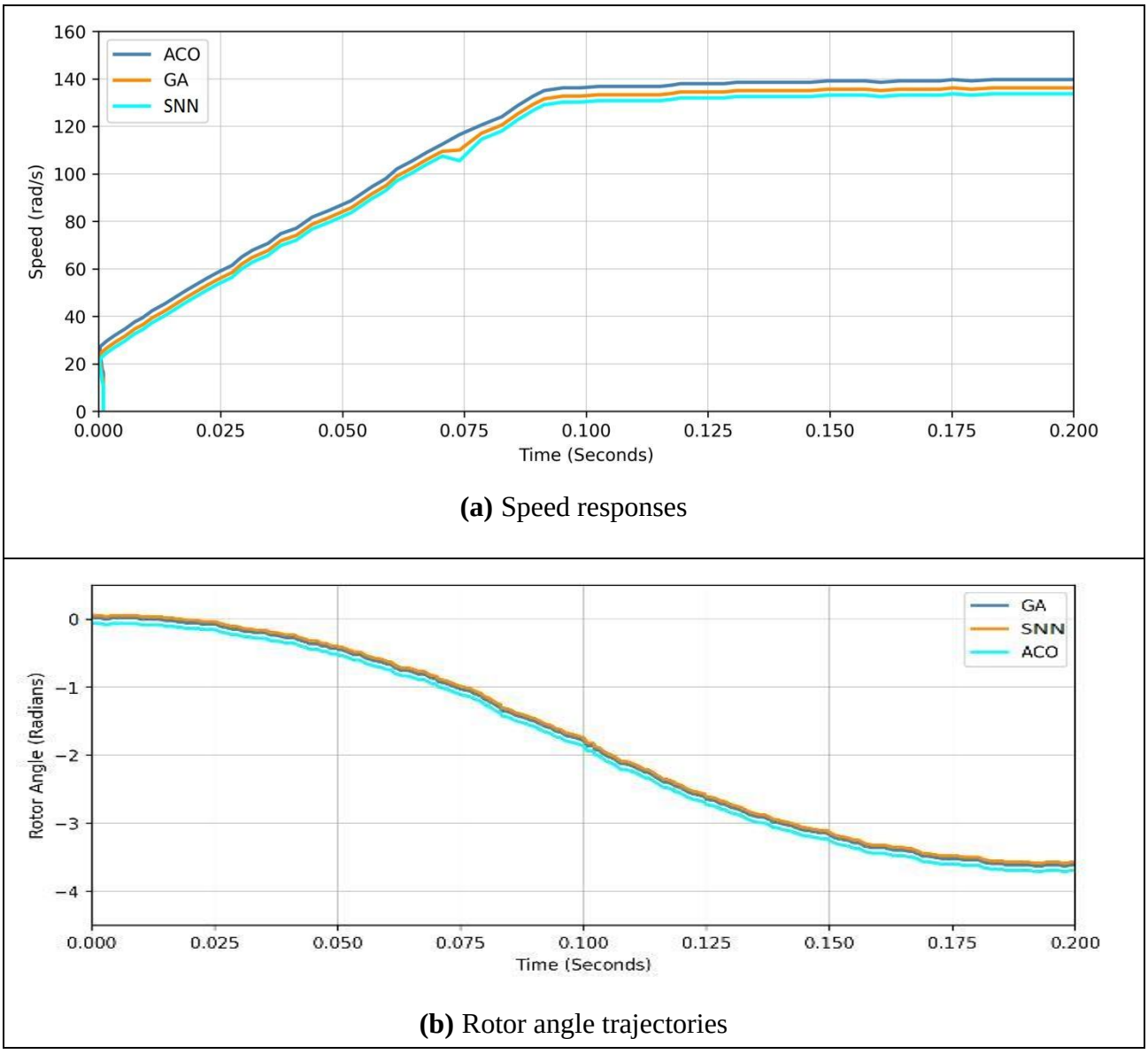

(a) Speed responses

(b) Rotor angle trajectories

Figure 11. Angular speed and rotor angle characteristics of ACO, GA, and SNN algorithm.

Figure 11(a) illustrates the rotor speed of the PMSM over the same simulation period. Here again, the GA, SNN, and ACO algorithms present very similar profiles, indicating that each method is equally effective in regulating the motor's speed. The speed increases rapidly at first, indicating an acceleration phase, and then levels off, showing that the motor reaches a stable operating speed. This uniformity in the performances of GA, SNN, and ACO reflects their robustness in controlling the motor's speed, which is vital for applications where consistent rotational velocity is necessary. The lack of significant divergence between the control strategies in this aspect suggests that any of them could be suitable for tasks where steady-state speed regulation is paramount.

The plot in Figure 11(b) showcases the rotor angle performance of a permanent magnet synchronous motor (PMSM) when controlled by three different optimization algorithms: genetic algorithm (GA), sequential neural network (SNN), and ant colony optimization (ACO). The lines for GA, SNN, and ACO are closely overlapped, indicating a high degree of similarity in the rotor angle tracking capability of each algorithm throughout the time span of the simulation. The angle decreases almost linearly with time, suggesting a steady rotational speed. The tight convergence of the three lines implies that all algorithms achieve a similar level of performance in maintaining the desired rotor angle trajectory, which is critical for precise motor control in applications requiring synchronization and positioning accuracy.

5. Conclusions

The SNN-MPC model showcased promising results, indicating a significant enhancement in PMSM drive performance. The d-q axis current characteristics, torque and speed responses, and rotor angle trajectories forecasted from the portrayed optimal control methods, SNN, GA, and ACO, rejuvenate the enforcement of SNN-MPC scheme in modern day machine drive systems. The comparative analysis with GA and ACO algorithms revealed the model's proficiency in managing the motor's dynamic behavior with greater accuracy and efficiency. The seamless integration of SNN-MPC in diverse computational environments underscores its adaptability and the potential for real-world applications. Future work will focus on refining the model for even better performance and exploring its applicability to a wider range of motor control scenarios, pushing the boundaries of what is achievable in PMSM drive technology.

Author contributions

Shaswat Chirantan: Resources, Investigation, Validation, Formal Analysis, Writing – original draft; Bibhuti Bhusan Pati: Supervision; All authors: Conceptualization, Methodology. All authors have read and approved the final version of the manuscript for publication.

Use of AI tools declaration

The authors declare they have not used artificial intelligence (AI) tools in the creation of this article.

Acknowledgments

The authors would like to thank Veer Surendra Sai University of Technology, Burla, Sambalpur, India, for facilitating this work.

Conflict of interest

The authors declare no conflict of interest in this paper.

References

1. Wang L, Chai S, Yoo D, Gan L, Ng K (2015) *PID and Predictive Control of Electrical Drives and Power Converters using MATLAB/Simulink*, John Wiley & Sons. https://doi.org/10.1002/9781118339459
2. Zhang X, Zhao Z (2021) Multi-stage Series Model Predictive Control for PMSM Drives. *IEEE T Veh Technol* 70: 6591–6600. https://doi.org/10.1109/TVT.2021.3086532
3. Ren B, Chen H, Zhao H, Xu W (2017) MPC-based torque control of permanent magnet synchronous motor for electric vehicles via switching optimization. *Control Theory Technology* 15: 138–149. https://doi.org/10.1007/s11768-017-6193-z
4. Liu M, Chan KW, Hu J, Xu W, Rodriguez J (2019) Model predictive direct speed control with torque oscillation reduction for PMSM drives. *IEEE T Ind Inform* 15: 4944–4956. https://doi.org/10.1109/TII.2019.2898004
5. Tan LN, Pham TC (2021) Optimal Tracking Control for PMSM With Partially Unknown Dynamics, Saturation Voltages, Torque, and Voltage Disturbances. *IEEE T Ind Electron* 69: 3481–3491. https://doi.org/10.1109/TIE.2021.3075892
6. Liu Z, Han Y, Feng G, Kar NC (2022) Efficient Nonlinear Multi-Parameter Decoupled Estimation of PMSM Drives Based on Multi-State Voltage and Torque Measurements. *IEEE T Energy Conver* 38: 321–331. https://doi.org/10.1109/TEC.2022.3187130
7. Marulasiddappa HB, Pushparajesh V, Begum A (2023) Direct Torque Control Based Jelly Fish Algorithm For Torque Ripple Reduction in Permanent Magnet Synchronous Motor. *2023 International Conference on Network, Multimedia and Information Technology (NMITCON)*, 1–6.
8. Kakodia SK, Giribabu D, Ravula RK (2022) Torque Ripple Minimization using an Artificial Neural Network based Speed Sensor less control of SVM-DTC fed PMSM Drive. 2022 *IEEE Texas Power and Energy Conference (TPEC)*, 1–6. https://doi.org/10.1109/TPEC54980.2022.9750850
9. Wang F, Zuo K, Tao P, Rodriguez J (2020) High performance model predictive control for PMSM by using stator current mathematical model self-regulation technique. *IEEE T Power Electron* 35: 13652–13662. https://doi.org/10.1109/TPEL.2020.2994948
10. Zhang Y, Jiang H, Yang H (2020) Model Predictive Control of PMSM Drives Based on General Discrete Space Vector Modulation. *IEEE T Energy Conver* 36: 1300–1307. https://doi.org/10.1109/TEC.2020.3036082
11. Favato A, Carlet PG, Toso F, Torchio R, Bolognani S (2021) Integral Model Predictive Current Control for Synchronous Motor Drives. *IEEE T Power Electron* 36: 13293–13303. https://doi.org/10.1109/TPEL.2021.3081827
12. Li Y, Xiao H, Jin N, Yan G (2022) Model predictive control of NPC three-level grid-tied converter based on reconstructed current. *Archives of Electrical Engineering* 71. https://doi.org/10.1109/ACCESS.2021.3119566
13. Agoro S, Husain I (2021) Robust Deadbeat Finite-Set Predictive Current Control With Torque Oscillation and Noise Reduction for PMSM Drives. *IEEE T Ind Appl* 58: 365–374. https://doi.org/10.1109/TIA.2021.3130022
14. Cui J, Tao T, Zhao W (2023) Optimized Control Set Model Predictive Control for Dual Three-Phase PMSM With Minimum Error Duty Cycle Regulation. *IEEE T Power Electr* 39:

1319–1332. https://doi.org/10.1109/TPEL.2023.3324209
15. Hassan M, Ge X, Atif R, Woldegiorgis AT, Mastoi MS, Shahid MB (2022) Computational efficient model predictive current control for interior permanent magnet synchronous motor drives. *IET Power Electronics* 15: 1111–1133. https://doi.org/10.1049/pel2.12294
16. Hassan M, Ge X, Woldegiorgis AT, Mastoi MS, Shahid MB, Atif R, et al. (2023) A look-up table-based model predictive torque control of IPMSM drives with duty cycle optimization. *ISA T* 138: 670–686. https://doi.org/10.1016/j.isatra.2023.02.007
17. Yao C, Sun Z, Xu S, Zhang H, Ren G, Ma G (2022) ANN Optimization of Weighting Factors Using Genetic Algorithm for Model Predictive Control of PMSM Drives. *IEEE T Ind Appl* 58: 7346–7362. https://doi.org/10.1109/TIA.2022.3190812
18. Li Y, Guo W, Liu D, Zhang X, Deng Y (2023) Model Predictive Current Control for Permanent Magnet Synchronous Motor based on Neural Network. 2023 *IEEE International Conference on Predictive Control of Electrical Drives and Power Electronics (PRECEDE)*, 1–6. https://doi.org/10.1109/PRECEDE57319.2023.10174503
19. Mao H, Tang X, Tang H (2022) Speed control of PMSM based on neural network model predictive control. *Tran Inst Meas Control* 44: 2781–2794. https://doi.org/10.1177/01423312221086267
20. Valdez F, Vázquez JC, Melin P (2021) A New Hybrid Method Based on ACO and PSO with Fuzzy Dynamic Parameter Adaptation for Modular Neural Networks Optimization. *Fuzzy Logic Hybrid Extensions of Neural and Optimization Algorithms: Theory and Applications*, 337–361. https://doi.org/10.1007/978-3-030-68776-2_20
21. Saeed IK, Sheikhyounis K (2022) Power quality improvement of distribution systems asymmetry caused by power disturbances based on particle swarm optimization-artificial neural network. *Int J Electr Comput Eng Syst* 25: 666–679. https://doi.org/10.11591/ijeecs.v25.i2.pp666-679
22. Chafi ZS, Afrakhte H (2021) Short-Term Load Forecasting Using Neural Network and Particle Swarm Optimization (PSO) Algorithm. *Math Probl Eng* 2021: Article ID 5598267. https://doi.org/10.1155/2021/5598267
23. Alhmoud L (2019) Short-term load forecasting for Jordan's Power System Using Neural Network based Different Optimization Techniques. *2019 IEEE International Conference on Environment and Electrical Engineering and 2019 IEEE Industrial and Commercial Power Systems Europe (EEEIC/I&CPS Europe)*, 1–6.
24. Abdolrasol MGM, Hussain S, Ustun T, Sarker M, Hannan M, Mohamed R, et al. (2021) Artificial Neural Networks Based Optimization Techniques: A Review. *Electronics* 10: 2689. https://doi.org/10.3390/electronics10212689
25. Moayedi H, Bui D, Gör M, Pradhan B, Jaafari A (2019) The Feasibility of Three Prediction Techniques of the Artificial Neural Network, Adaptive Neuro-Fuzzy Inference System, and Hybrid Particle Swarm Optimization for Assessing the Safety Factor of Cohesive Slopes. *ISPRS Int J Geo-Inf* 8: 391. https://doi.org/10.3390/ijgi8090391
26. Mahadeva R, Kumar M, Manik G, Patole S (2021) Modeling, simulation, and optimization of the membrane performance of seawater reverse osmosis desalination plant using neural network and fuzzy based soft computing techniques. *Desalin Water Treat* 229: 17–30. https://doi.org/10.5004/dwt.2021.27386
27. Jayalakshmi M, Rao S (2020) Discrete Wavelet Transmission and Modified PSO with ACO

Based Feed Forward Neural Network Model for Brain Tumour Detection. *CMC-Comput Mater Continua* 65: 1081–1096. https://doi.org/10.32604/cmc.2020.011710

28. de Jesus KLD, Senoro D, dela Cruz JD, Chan E (2021) A Hybrid Neural Network–Particle Swarm Optimization Informed Spatial Interpolation Technique for Groundwater Quality Mapping in a Small Island Province of the Philippines. *Toxics* 9: 273. https://doi.org/10.3390/toxics9110273
29. Krishna K, Thirumuru R (2023) Enhanced QOS energy-efficient routing algorithm using deep belief neural network in hybrid falcon-improved ACO nature-inspired optimization in wireless sensor networks. *Neural Netw World* 33: 113–141. https://doi.org/10.14311/nnw.2023.33.008
30. Chirantan S, Pati BB (2024) Torque and dq axis current dynamics of an inverter fed induction motor drive that leverages computational intelligent techniques. *AIMS Electronics and Electrical Engineering* 8: 28–52. https://doi.org/10.3934/electreng.2024002
31. Dat NT, Kien CV, Anh HPH (2021) Hybrid Super-Twisting Sliding Mode and FOC Scheme for Advanced PMSM Driving Control. *International Conference on Advanced Mechanical Engineering, Automation, and Sustainable Development*, 776–780. https://doi.org/10.1007/978-3-030-99666-6_112
32. Sahu S, Nayak B, Dash RN (2022) Analysis of Five-Phase Surface PMSM for Application in Electric Vehicles. *Sustainable Energy and Technological Advancements: Proceedings of ISSETA 2021*, 587–595. https://doi.org/10.1007/978-981-16-9033-4_43

AIMS Press